

Simulation of Thermal Stability and Friction: A lubricant confined between Monolayers of Wear Inhibitors on Iron Oxide

T. Çağın^{1,*}, Y. Zhou¹, E. S. Yamaguchi², R. Frazier²,
A. Ho², Y. Tang³, and W. A. Goddard, III¹

1) Materials and Process Simulation Center, 139-74
California Institute of Technology, Pasadena, California 91125

2) Chevron Chemical Company, 100 Chevron Way, Richmond, California 94802

3) Chevron Petroleum Technology Company, 1300 each Boulevard,
La Habra, California 90631

Abstract

To understand antiwear phenomena in motor engines at the atomic level and provide evidence in selecting future ashless wear inhibitors, we studied the thermal stability of the self-assembled monolayer (SAM) model for dithiophosphate (DTP) and dithiocarbamate (DTC) molecules on the iron oxide surface using molecular dynamics. The interactions for DTP, DTC and Fe_2O_3 are evaluated based on a force field derived from fitting to *ab initio* quantum chemical calculations of dimethyl DTP (and DTC) and $\text{Fe}(\text{OH})_2(\text{H}_2\text{O})_2$ -DTP (DTC) clusters. MD simulations at constant-NPT are conducted to assess relative thermal stabilities of the DTP and DTC with different pendant groups (n-propyl, i-propyl, n-pentyl, and i-pentyl). To investigate frictional process, we employ a steady state MD method, in which one of the Fe_2O_3 slabs maintained at a constant linear velocity. We obtain the time averaged normal and frictional forces from the interatomic forces. Then, we calculated the friction coefficient at the interface between SAMs of DTP and the confined lubricant, hexadecane, to assess the shear stability of DTPs with different pendant groups.

1 Introduction

Zinc dithiophosphates (ZnDTP) have been used for several decades¹ to reduce wear to acceptable levels in modern engines. Although DTP is the most effective and economic antiwear agent used, there is environmental concern due to the level of phosphorous content in the formulation. Finding a ZnDTP replacement with lower phosphorus content and providing the necessary wear protection to engine surfaces is very important for the oil industry. One might consider other lubricant additives which are presently used to control friction, deposits, corrosion, oxidation, and rust (for a review, see reference 2). However, the number of possible chemical compounds is enormous, making an empirical search laborious and expensive. It should also be noted that a single complete engine test for a new wear inhibitor costs around \$150,000. Another serious impediment to this search is that the factors underlying good wear performance are not well understood.

Using atomistic level modelling and molecular dynamics (MD) simulation to provide guidance in prioritizing new materials for experimental testing is a viable alternative. For instance, our earlier work led to a self-assembled monolayer (SAM) model, where we found the calculated cohesive energy of the wear inhibitor correlates inversely with wear performance.^{3,4}

The purpose of a lubricant is to provide a protective coating to the solid surfaces. This, in turn prevents formation of adhesive junctions, reduces frictional energy losses by acting as an interfacial layer of low shear strength. Our understanding of the friction of two solid surfaces sliding against each other with a thin liquid film between them has been greatly advanced over the last ten years. The work on a variety of

different surfaces, such as mica, silica, metal oxide, and surfactant monolayer surfaces, sliding across different lubricants have shown that the properties of fluids confined to the nanometer scale are very different from the bulk properties. For example, the “effective” viscosity of a thin lubricant film is often much higher than bulk viscosity.

In this paper, extending our earlier work on the SAM model of wear inhibitors^{3,4}, we calculated the adsorption energies and coverage for DTP and DTCs at 500 K. We found that for DTP the SAM model of adsorption energies correlate (inversely) with wear obtained from engine tests. We also present results of molecular dynamics simulations of shear stability of these SAM in the presence of lubricant (normal-hexadecane). The lubricant is confined by two iron-oxide solid surfaces on which DTP molecules are chemisorbed to form a self-assembled monolayer. We have carried out the simulations for three different DTP molecules: isopropyl (i-Pr), isobutyl (i-Bu), and phenyl (Phe) to investigate the effect of the SAMs on the dynamic properties of the lubricant.

2 Simulation Results and Discussion

2.1 The Force Fields for DTP, DTC and Iron Oxide.

We modified the universal force field (UFF)⁵ parameters to fit the *ab initio* calculations, (geometry, bond energy, and vibrational frequency from HF calculations on clusters containing DTP bonded to the metal) for this work.

The total potential energy of the system is given by

$$E = E_{val} + E_{nb} \quad (1)$$

The valence interactions, $E_{val} = E_{bond} + E_{angle} + E_{torsion} + E_{inversion}$, consist of bond stretch (E_{bond}), bond-angle bend (E_{angle}), dihedral angle torsion ($E_{torsion}$), and inversion ($E_{inversion}$) terms. For E_{bond} we use Morse terms, for angle terms we use the dihedral cosine harmonic terms. For $E_{torsion}$ we use $E_{torsion} = \frac{1}{2} V_3 (1 + \cos 3\phi)$ and for the inversion energy, we have used the harmonic expression: $E_{inv} = K_i (\psi - \psi_0)^2$.

The nonbonded interactions, E_{nb} , consist of vdw (E_{vdw}) and electrostatic (E_Q) terms, for E_{vdw} we use exponential-6 and Morse terms. The equilibrium bond lengths (R_0) and angles (θ_0) were fitted to the *ab initio* geometries. The force constants (i.e. K_b , K_θ , etc.) were fitted to the *ab initio* vibrational frequencies using the biased Hessian method.⁶ The torsional barriers (V_m) were adjusted to reproduce the conformational energy differences from the HF calculations. For metal-DTP (-DTC) systems the Fe-S interaction was treated as a nonbonded interaction just as for the Zn-S interactions of ZnDTP systems.³ That is, they were described with vdw and electrostatic terms only (no valence terms). This allows DTP (or DTC) to dissociate smoothly from the metal surfaces. The further details and parameters are given in References 3 and 4.

2.2 Self Assembled Monolayer and Adsorption at Different Coverage

The simulation results presented below are mainly from two types of calculations: one from minimized structures and the other from MD simulations at 500 K using NVT ensemble molecular dynamics. The run times of simulation vary between 10 ps and 20 ps. The integration time step is 1 fs.

To determine the adsorption energy, we first calculate the cohesive energy as a function of the number of molecules adsorbed,

$$E_{coh} = -(E_{surf+SAM} - E_{surf} - N \times E_{mol}) \quad (2)$$

where $E_{surf+SAM}$, E_{surf} , and E_{mol} are the total energy of the Fe_2O_3 surface plus SAM, that of the Fe_2O_3 surface only, and that of the SAM molecule in the gas phase, respectively. The adsorption energy per molecule, E_{ad} , is then obtained from the ration of the cohesive energy to the number of adsorbate molecules.

The results for DTP are summarized in Figure 1, (a) from the minimized structures, and (b) from the dynamics simulations. Clearly, the adsorption energy curves in Figure 1 are quite flat when the number of adsorbate molecules is less than 8 (i.e., $\leq 1/2$ coverage). The errors in adsorption energy under our simulation conditions are estimated to be 1 kcal/mol/molecule. Within this error the adsorption energies up to 1/2 coverage can be considered more or less a constant. After 1/2 coverage, the adsorption energies begin to drop. The considerable reduction in adsorption energy indicates that the ligand-effect due to interaction between neighboring adsorbed molecules become significant when the surface coverage exceeds

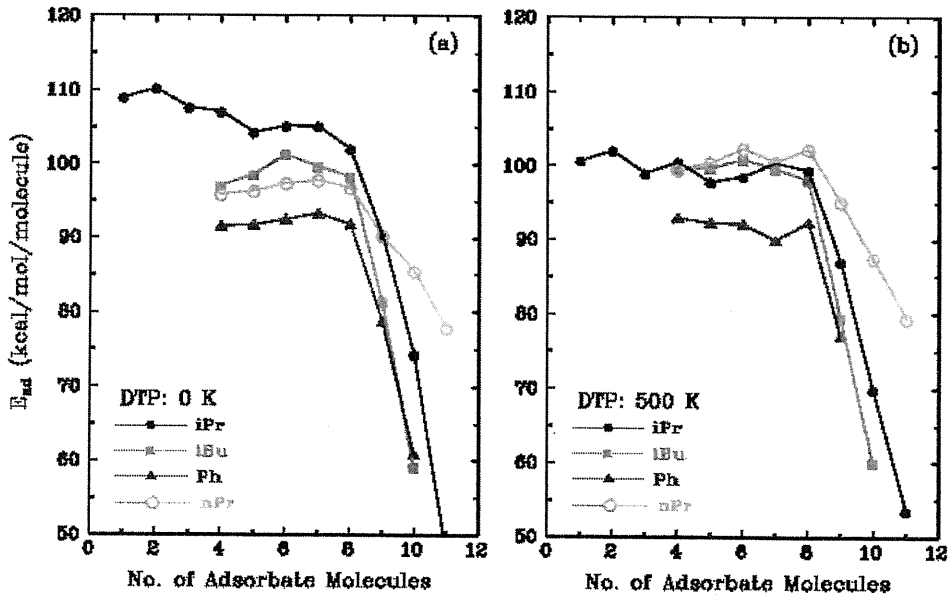


Figure 1: Adsorption energy as a function of surface coverage for DTP molecules: (a) from minimized structures; (b) from molecular dynamics simulations at 500 K. The adsorption energies remain almost a constant up to 1/2 coverage (i.e., 8 adsorbate molecules).

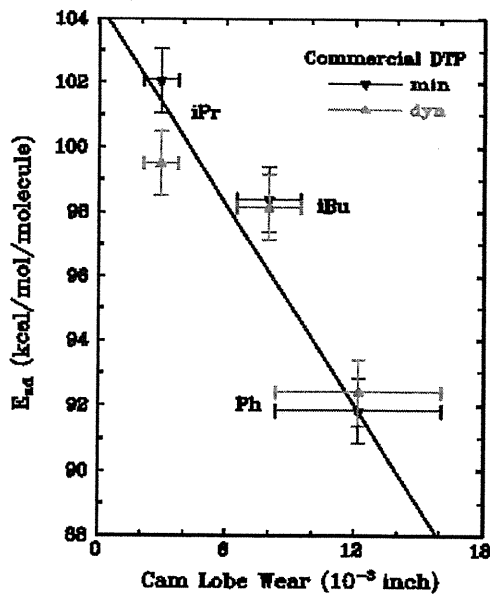


Figure 2: Correlation of SAM adsorption energy with wear in engine wear tests for commercial DTP molecules. The error in the adsorption energy is 1 kcal/mol/molecule. The straight line is the least-square fit to the results of both minimization and dynamics simulation.

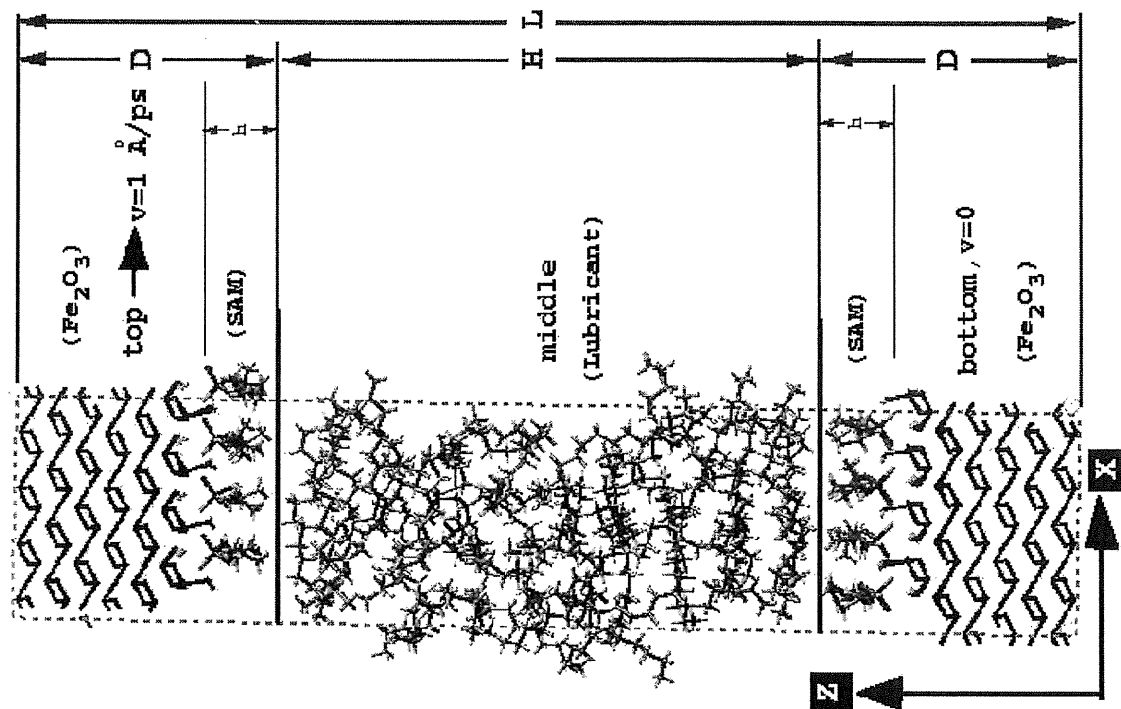


Figure 3: Friction simulation setup: 2-D periodic boundary conditions imposed in x- and y-directions. The top layer is driven at a constant velocity in x-direction.

1/2. Similar results are obtained for DTC. Here, the decrease in adsorption energy for these DTC molecules is more gradual, and it does not start exactly at 1/2 coverage in some cases. For example, for iso-heptyl (iC₇) and normal-heptyl (nC₇), the adsorption energies begin to decrease at 3/8 coverage. However, the molecular dynamics simulations of the monolayers of these DTC molecules show an enhancement in adsorption energy as the critical surface coverage increases to 1/2.

In Figure 2, we plotted the adsorption energy at 1/2 coverage against the measured maximum wear in engine wear tests⁷ for the three commercial R groups of DTP. Both the minimization and dynamics simulation results are shown. The straight line in the figure is the least-square fit to the both sets of data. We see that the adsorption energies correlate with the wear data. A stronger adsorbed monolayer provides a smaller wear and, hence, a better protection to the surface. This correspondence between the adsorption energy and wear presents a basis for predicting the antiwear performance of other materials prior to engine tests.

2.3 Friction and Shear Stability of SAM-Lubricant Interface

To simulate the the shear stability and the friction between the SAM of wear inhibitors and lubricant, we considered the model system shown in Figure 3. The fluid portion, consisting of 32 molecules of C₁₆H₃₄, is sandwiched between two planar walls. Each wall is made of an hexagonal iron-oxide (0001) surface and a monolayer of DTP molecules; the binding between the surface and SAM is through chemisorption. The geometrical parameters for this set up are, $D = 2$ nm, $H = 4.4-4.5$ nm, and $h=0.6-0.7$ nm depending on the type of SAM used. L , is around 8.5 nm, the actual value is determined by the energy minimization of the entire system for each case.

Simulations aimed at generating planar Couette flow by moving the top wall at a constant velocity v along the X axis while holding the lower wall fixed. In the results presented below, $v = 1$ Å/ps. 2-dimensional periodic BC's are imposed along the X and Y directions. In all simulations, the time step is 1 fs. The duration of runs are 200 ps. The trajectories are stored every 0.05 ps for analysis.

In order to capture the stick-slip motion, we used *the displacement* over a 5 ps interval to derive the

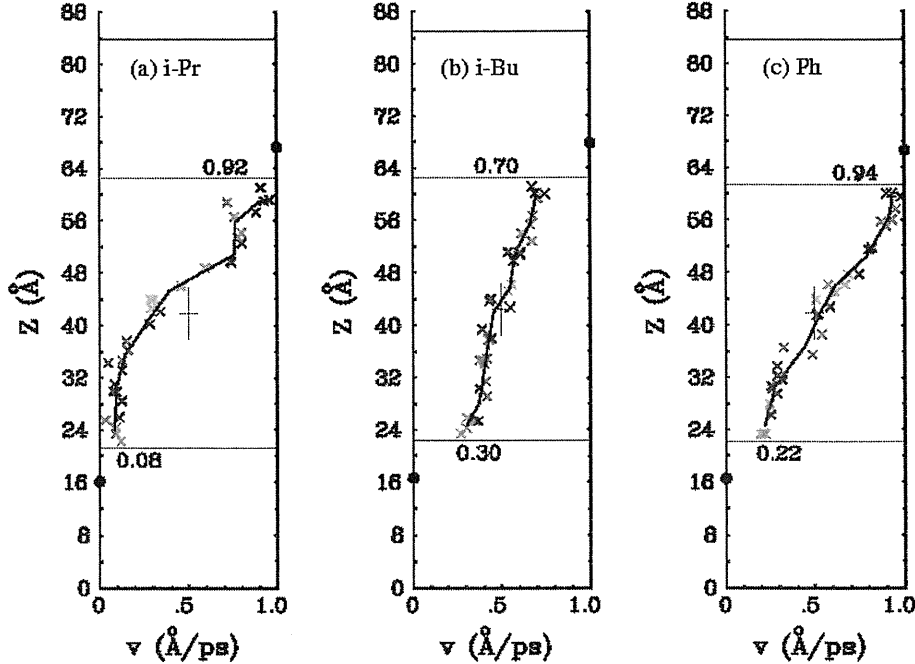


Figure 4: Velocity profile for a) i-Pr, b) i-Bu and c) Phe. The crosses are the average streaming velocity for each molecule, the solid line is the average over the number of molecules

streaming velocity of the molecules. The streaming velocity of each molecule is calculated from a linear least-square fit. This procedure gives a smooth streaming velocity profile as a function of time for each molecule. The resulting velocity profiles for each case studied (i-Pr, i-Bu, Phe) are shown in Figure 4. The solid line in each panel is the velocity of the layer (8-layers constructed along Z-direction) averaged over time and over the number of the molecules in that layer. The crosses on each panel represent the streaming velocity of each molecule.

It is apparent that the different characteristics in velocity profile have resulted from the difference of the strength of interactions at the lubricant-SAM interfaces. Now we look at the slip, or the velocity differences between fluid and wall, at the interfaces. We can see that the slip for i-Bu is larger than those for i-Pr and Phe. The slip at the wall-fluid interface is one of issues heavily investigated by previous simulations because of its relevance to the boundary condition in fluid dynamics. A broad spectrum of boundary conditions was observed ranging from pure slip to complete no-slip (locking). The degree of slip at the boundary depends on several interfacial parameters including the strength of the liquid-solid coupling, the thermal roughness of the interface, and the commensurability of wall and liquid densities. For i-Pr, the profiles indicate a plug-flow at initial times, *i.e.*, the entire fluid is dragged along by the top wall. This over-shooting is gradually relaxed in later times. After 100 ps, the velocity profile approaches a steady-state. This kind of flow overshooting is much less profound for Phe, and it is inexistent for i-Bu.

2.4 Properties: Friction Coefficient and Apparent Viscosity

The normal and friction forces acting on the fluid due to the interactions from the top and bottom walls are calculated for each run (i-Pr, i-Bu, and Phe) to determine the friction coefficient and apparent viscosity.

It seems that there is a slight increase in the force in the normal direction over time. This may be caused by the increase in temperature of the lubrication during the dynamic. In these simulations, we did not implement Langevin bath to maintain the temperature of each region. So that we could also calculate the friction force from the slope of the work done as a function of time. The two methods of deriving friction force, from direct evaluation or from the slope of the work, give the consistent results on the friction force.

The friction coefficient is calculated from the ratio of the normal force and friction force:

$$\mu = \frac{F_x}{F_z} \quad (3)$$

The results are 0.143 ± 0.001 , 0.124 ± 0.00 and 0.135 ± 0.001 nN for i-Pr, i-Bu and Phe cases, respectively. It is seen that the friction coefficient is largest for i-Pr, smallest for i-Bu, and falls in between for Phe. But the differences may be insignificant given the uncertainties.

It is interesting to note that the ordering in friction coefficient is coincident with that in the thickness of SAM. It is possible that a thicker SAM diminishes corrugation of the underlying surface more so that the friction coefficient is reduced when the DTP molecules with longer hydrocarbons are chemisorbed to the surface.

In experiments the effective viscosity is calculated from the measured shear stress and the applied shear rate with the assumption of linear velocity profile via

$$\eta = \frac{\sigma}{(\partial v / \partial z)} \quad (4)$$

where σ is the shear stress and $(\partial v / \partial z)$ is the shear rate. The shear stress in our systems are obtained from the friction force divided by the area of the surface. Since the velocity profile in our simulations is not linear in some cases, we use the velocity gradient at the top interface to estimate the effective viscosity of the lubricant close to the top interface. For a direct comparison, the friction forces of different SAMs are normalized to the same normal force. The apparent viscosities calculated are, 2.68, 2.36, 2.41 mPa.s (cP) for i-Pr, i-Bu and Phe respectively.

In all cases we studied, the surfaces are covered by a chemisorbed perfect SAM of wear inhibitors and a layer of lubricant. In our simulations no wear (large friction and consequently wear) was observed. However, if the two surfaces were in direct contact in some region, due to asperities, the high friction could have been strong enough to tear them apart.

3 Concluding Remarks

Assessment of a new material demands the choice of a suitable criterion that can distinguish promising materials from those with little potential. For wear inhibitors, the key parameters that we considered are the adsorption energy at minimization and at elevated temperatures, and the shear resistance under frictional conditions. In this paper we presented such an assessment based on molecular dynamics simulations. We observed that the adsorption energies calculated from molecular dynamics simulations at 500 K correlate with the wear data. This correlation between the adsorption energy and measured wear can be used for predicting the antiwear performance of other materials prior to engine tests.

ACKNOWLEDGEMENT: This research was funded by grants from Chevron Chemical Company. The facilities of MSC is also supported by funds from NSF, DOE-ASCI, ARO/DURIP, ARO-MURI, ONR; Asahi Chemical, Avery Dennison, BP Chemical, Beckman Institute, Chevron Petroleum Technology Co., Chevron Chemical Co., Exxon, Owens Corning and Seiko-Epson.

REFERENCES

1. H. C. Freuler, *U.S. Patent* 2364283, 1944.
2. T. V. Liston, T. V. *J. Soc. Trib. Lub. Eng. May*, 389 (1992).
3. S. Jiang, S. Dasgupta, M. Blanco, R. Frazier, E. S. Yamaguchi, Y. Tang, and Goddard, W. A., III *J. Phys. Chem.* **100**, 15760 (1996).
4. S. Jiang, R. Frazier, E. S. Yamaguchi, M. Blanco, S. Dasgupta, Y. Zhou, T. Çağın, Y. Tang, and Goddard, W. A., III *J. Phys. Chem.* **101**, 7702 (1997).
5. A. K. Rappé, C. J. Casewit, K. S. Colwell, W. A. Goddard, W. M. Skiff *J. Am. Chem. Soc.* **114**, 10025 (1992).
6. S. Dasgupta, W. A. Goddard III, *J. Chem. Phys.* **90**, 7207 (1989).
7. S. H. Roby, *Lubr. Eng.* **47**, 413 (1991). M. T. Benchaita, *Lubr. Eng.* **47**, 893 (1991).